

HPLC, UV–vis and NMR spectroscopic and DFT characterization of purpurin isolated from *Rubia tinctorum* L.

Zoran S. Marković¹, Nedeljko T. Manojlović², Svetlana R. Jeremić¹, Miroslav Živić³

¹State University of Novi Pazar, Department of Chemical–Technological Sciences, Novi Pazar, Serbia

²University of Kragujevac, Faculty of Medicinal Sciences, Department of Pharmacy, Kragujevac, Serbia

³University of Belgrade, Faculty of Biology, Belgrade, Serbia

Abstract

Purpurin (1,2,4-trihydroxyanthraquinone), a naturally occurring anthraquinone pigment present in the root of *Rubia tinctorum* (Mull. Arg.) Zahlbr. was isolated from the plant, purified and characterized by HPLC chromatography, UV-vis and NMR spectroscopy. The geometries of the purpurin conformers were optimized using the B3LYP/6-311+G(d,p) level of theory. It was found that all conformations have similar energies and that the corresponding purpurin radicals are planar. In spite of their planarity, there is no significant electron delocalization over the A and C rings. The antioxidant properties of purpurin were investigated using the colorimetric assay as Trolox-equivalent antioxidant capacity, and theoretical BDE (Bond Dissociation Enthalpy). Both methods revealed that purpurin has strong antioxidant capacity.

Keywords: *Rubia tinctorum*, HPLC-UV, antioxidant activity, anthraquinone, DFT study.

Available online at the Journal website: <http://www.ache.org.rs/HI/>

SCIENTIFIC PAPER

UDC 547.673:58:543.42

Hem. Ind. 67 (1) 77–88 (2013)

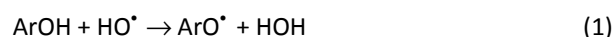
doi: 10.2298/HEMIND120419058M

Anthraquinones are the largest and most important group of naturally occurring quinones. They are used as natural and synthetic color and are constituents of plants used for dyeing materials [1]. Many plants contain anthraquinones are used as pharmaceutical drugs [2,3]. Numerous anthraquinones have a linear tricyclic ring framework, with various number of phenolic functional groups. A wide range of biological and pharmacological activities of anthraquinones, such as antimicrobial, antiviral, anti-inflammatory, anti-cancer, antioxidant, and antifungal [4–11] depend on their tricyclic scaffold, and on the nature and/or positions of substituents [12]. As anthraquinones have similar structure as flavonoids, a similar approach can be applied. Herbs containing anthraquinone derivatives are used as laxatives. The root of *Rubia tinctorum* (madder) is the source of natural anthraquinone dyes, including the most important alizarin and purpurin. Besides alizarin and purpurin, 35 other anthraquinone glycosides and aglycons have been reported as constituents of this plant [13]. The anthraquinones found in *Rubia tinctorum* differ in the nature of their substituents and in their substitution pattern.

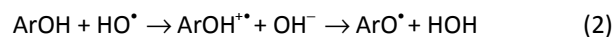
Recent scientific studies have confirmed that purpurin, alizarin and their derivatives possess biological activity including antimicrobial and cytotoxic activities, and also have a strong inhibitory effect on the genotoxicity of several carcinogens [14–17]. Extract of *Rubia*

tinctorum has been used for treatment of kidney and bladder stones [18,19]. Several screening methods of anthraquinones in *Rubia tinctorum* L., based on reversed-phase high-performance liquid chromatography (RP-HPLC) have been described in literature [12,20].

There are two basic and most applicable reaction pathways through which free radicals (ArO[•]) are formed from anthraquinones (ArOH). The first includes rapid hydrogen atom donation to a present radical (1), through which a new radical, more stable than the initial one, is formed (Hydrogen Atom Transfer-mechanism – HAT), leading to the direct OH bond breaking.



The second reaction pathway is Proton-Coupled Electron Transfer (PCET) mechanism (2), by which the primary antioxidant transforms into radical cation, donating an electron to a free radical present in the system (e.g. lipid or some other radical). This mechanism leads to indirect H-abstraction.



In the HAT mechanism the proton and electron are transferred together, whereas in the PCET mechanism the proton and electron are transferred between different sets of molecular orbitals [21–24]. The net result of both reactions is the same. The reactions occur in parallel by different rates. Many important biochemical processes obey the above mentioned mechanisms.

Both HAT and PCET mechanisms have been the subject of investigation. Which mechanism will be dominant in a given reaction depends on the phenolic OH

Correspondence: N. Manojlović, Department of Pharmacy, Medical Faculty, University of Kragujevac, 34000 Kragujevac, Serbia.

E-mail: ntm@kg.ac.rs

Paper received: 19 April, 2012

Paper accepted: 28 May, 2012

bond strengths. The OH bond strength can be expressed as the OH bond dissociation enthalpy (*BDE*). This molecular property can be used in the assessment of possible radical scavenging potential of the molecule. *BDE* is calculated as the difference between the molecule (purpurin in this case) and its radical enthalpies. Density functional theory (DFT) often produces reliable results on the *BDE* with relatively reasonable computational cost [25–36]. It is worth pointing out that the small *BDE* value means that the OH bond is weak, and that the reaction will probably obey the fast HAT mechanism. On the other hand, in the PCET mechanism, the ionization potential of ArOH plays an important role, because the rate of formation of ArOH⁺• determines the rate of the overall reaction. Whichever mechanism is operative, removing a hydrogen atom from ArOH needs to be easier than that from HOH. This means that both reactions (1) and (2) should be thermodynamically favorable, and that the formed radical species ArO• needs to be relatively stable. In this way, the antioxidant molecule prevents or postpones toxic effects of radicals (such as the oxidative stress), slowly reacting with the substrate and faster with the present radicals. In these reactions, neither the antioxidant molecule nor the final product obtained from it have toxic or pro-oxidant effects [37].

The first part of this work is devoted to HPLC characterization of *Rubia tinctorum* L. specimens collected in central Serbia, isolation of major pigment, purpurin, and its characterization by UV–vis and NMR spectroscopy, and determination of its antioxidant capacity. In addition, a DFT study on the reactivity of the OH groups in purpurin and the structural and electronic features of the purpurin radicals were performed. The results for *BDE*, HOMO, and spin density of purpurin are presented. Structure-activity relationships are examined in the light of these results. Particular attention is devoted to the DFT interpretation of the reactivity of the OH groups in purpurin and the radicals formed after H removal from this molecule. Keto-enol tautomerism before H-abstraction is also discussed to explain the role of the OH groups.

EXPERIMENTAL

Chemical reagents

All reagents used in the experiment were analytical grade in the highest purity available. Acetonitrile was of HPLC grade, and was purchased from Merck (Darmstadt, Germany). Deionized water used throughout the experiments was generated by a Milli-Q academic water purification system (Milford, MA, USA).

Plant material

Plant material was collected from Central Serbia (10 km south of the Arandjelovac town) during July, 2008.

The studied plant was identified by Prof. Dr. Vasiljević, Department of Biology, Faculty of Science, University of Niš, Serbia, as *Rubia tinctorum* (L.) (voucher specimen UNI-2403).

Preparation of plant extract and isolation of purpurin

The plant material was air dried at room temperature (26 °C) for one week, after which it was grinded to a uniform powder. After extraction with methanol the residue was hydrolysis with 2 mol/L HCl, neutralized with solution NaOH and extracted with methanol. After evaporation of the solvent, the residue was partitioned between chloroform and water. The chloroform fraction was extracted with 1 mol/L NaOH, which was then acidified with HCl and extracted with chloroform. This extract was chromatographed on Sephadex LH-20 (eluent chloroform-methanol 20:1, 10:1, 5:1 and 1:1) to yield purpurin which was identified according to spectral data [38]. Purpurin is a crystalline solid that forms red needles melting at 260 °C.

High-performance liquid chromatography (HPLC) analysis

High-performance liquid chromatography (HPLC) analysis was carried out on an Agilent 1200 Series HPLC instrument with C18 column (C18; 25 cm×4.6 mm, 10 μm) and UV–vis spectrophotometric detector with two solvents, water and acetonitrile, in a linear gradient program (Table 1). The sample injection volume was 10 μL. The flow rate of the mobile phase was kept constant at 1.0 mL min⁻¹ and the chromatogram was recorded at 250 nm while the UV spectra were monitored over a range of 600 to 200 nm. Purpurin was identified by comparison of its retention time and absorption spectrum to this of standard solution of purpurin.

Table 1. Gradient table for HPLC analysis

Time, min	Water, %	Acetonitrile, %
0	70	30
5	75	25
20	40	60
30	30	70
40	75	25
45	70	30

NMR Spectra

The ¹H- and ¹³C-NMR spectra of purpurin were recorded at room temperature on a Bruker NMR spectrometer (500 MHz for ¹H- and 125 MHz for ¹³C-NMR). TMS was used as internal standard. The samples were prepared by the dissolution of purpurin in DMSO (signal for ¹H- at 2.5 ppm and at 39.5 ppm for ¹³C-NMR).

Antioxidant activity

The 2,2'-azinobis-(3-ethylbenzothiazoline-6-sulphonic acid) (ABTS) and 6-hydroxy-2,5,7,8-tetramethylchroman-2-carboxylic acid (Trolox) were obtained from Fluka (Switzerland). The total antioxidant activity of purpurin was determined by the colorimetric assay as Trolox-equivalent antioxidant capacity (TEAC). The stable ABTS radical monocation (ABTS^{•+}) was generated by the incubation of 7 mM ABTS with 2.5 mM potassium persulfate in the dark at room temperature for 16 h before use. The ABTS^{•+} solution was diluted immediately prior to assay to an absorbance of 0.70±0.02 at 734 nm. 500 µL of diluted ABTS^{•+} solution was placed in the quartz cuvette to record the initial absorbance. Then, various concentrations of purpurin or Trolox were added to each cuvette, mixed by inversion, and the absorbance was read exactly at 60 s after addition. Parallel blanks were performed in each assay with the appropriate solvent alone. The percentage inhibition compared to initial absorbance after 60 s was plotted as a function of sample or Trolox concentration. TEAC value was expressed as the ratio of sample and Trolox slope ($a_{\text{sample}}/a_{\text{Trolox}}$). Each assay was carried out in triplicate.

Computational method

All calculations were performed in vacuum, using Gaussian09 software package [39], at the B3LYP/6-311+G(d,p) level of theory [40]. Six different in-plane conformations of purpurin were found and investigated. The differences between conformations are in OH groups orientation at C1, C2, and C4 atoms. Obtained geometries were verified to be minima on the potential energy surface by a normal mode analysis – no imaginary frequencies were found. Transitions to the lowest excited singlet electronic states of purpurin were computed by using the TD-B3LYP procedure [40–42]. The influence of methyl alcohol as solvent upon the electronic transitions was approximated by the polarized continuum model PCM [43,44]. UV–vis spec-

tral analysis was performed using ChemCraft 1.5 [46], and Gausssum [45]. The calculation of NMR spectrum of purpurin was performed using the GIAO (Gauge-Including Atomic Orbitals) method [47,48], implemented in the Gaussian package. In order to express the chemical shifts in ppm, the geometry of the tetramethylsilane (TMS) molecule was optimized, and then its NMR spectrum was calculated by using the same method and basis set as for the calculation of purpurin molecule.

The obtained zero point energies were used to correct all energetic terms using the recommended scaling factor of 0.9887 [49]. Natural bond orbital (NBO) analysis [50] was performed for all structures. Bond dissociation enthalpy (*BDE*) for purpurin (Table 2) was calculated using the following equation:

$$BDE = H_{\text{POH}} - H_{\text{PO}^{\bullet}} - H_{\text{H}^{\bullet}}$$

where H_{POH} , $H_{\text{PO}^{\bullet}}$, and $H_{\text{H}^{\bullet}}$ present the enthalpy of purpurin, purpurin radical, and hydrogen atom, respectively. The ionization potential (IP) was obtained as the energy difference between the POH and POH^{•+} species.

RESULTS AND DISCUSSIONS

The HPLC chromatogram of the crude extract of *Rubia tinctorum* is shown in Figure 1. The t_{R} values for purpurin is 25.24 min. Beside purpurin, very important anthraquinone alizarin was also identified ($t_{\text{R}} = 23.64$ min). The identification of these compounds were performed by comparison of their t_{R} values with the standard substances. The UV–vis absorbance spectral results also correspond to the literature data [51]. Bearing in mind the importance of the pigment purpurin, this anthraquinone was isolated from the extract by column chromatography on silica gel. Purpurin contains three hydroxyl groups located in the same ring. These groups can play an important role in the expression of antioxidant activity of purpurin.

Table 2. Calculated energies of the purpurin rotamers (1 to 6), purpurin radicals (1-OH, 2-OH, and 4-OH, and keto forms of purpurin

Compound	Total energy, a.u.	Enthalpy, a.u.	Free energy, a.u.	BDE, kJ/mol
1	-914.5376	-914.5269	-914.5802	-
2	-914.5303	-914.5185	-914.5721	-
3	-914.5160	-914.5037	-914.5587	-
4	-914.5169	-914.5047	-914.5593	-
5	-914.5072	-914.4947	-914.5501	-
6	-914.4937	-914.4806	-914.5389	-
1-OH	-913.9010	-914.8891	-913.9441	362.15
2-OH	-913.8997	-913.8879	-913.9421	365.28
4-OH	-913.8862	-913.8741	-913.9294	401.58
Keto C-2	-914.4638	-914.4514	-914.5072	163.80
Keto C-11	-914.4940	-914.4822	-914.5363	244.68

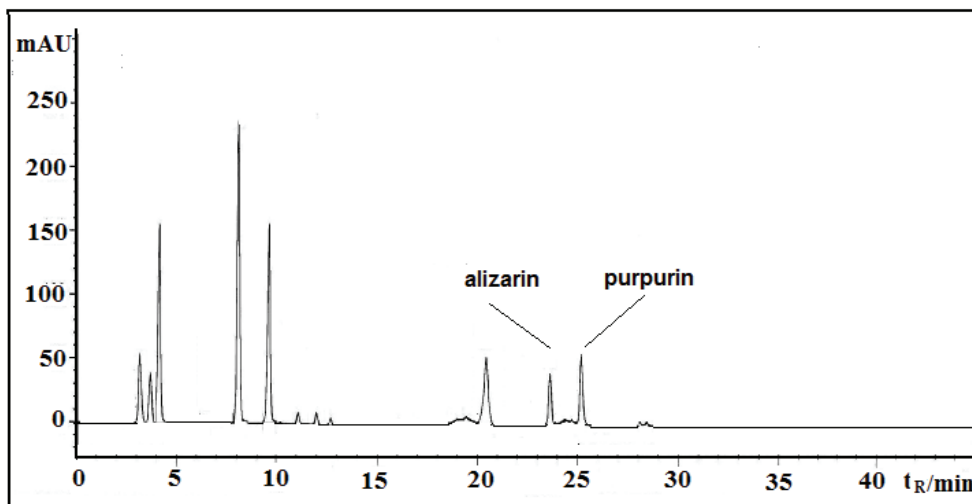


Figure 1. HPLC Chromatogram of the *Rubia tinctorum* specimen.

To find the most stable conformation of purpurin, which will be used for further investigations, the conformational space of purpurin was explored as a function of the torsion angles τ_1 (C2-C1-O1-H), τ_2 (C3-C2-O2-H) and τ_3 (C3-C4-O4-H). In this way, the preferred relative positions among OH groups in relation to benzene ring were determined. The minimization procedure yielded a planar conformation ($\tau_1 = \tau_2 = \tau_3 = 180^\circ$)

as the most stable structure (**1** in Figure 2). By removing constraint for the torsion angles, the conformational absolute minimum was found at ($\tau_1 = \tau_2 = \tau_3 = 180^\circ$). Five local minima were also found, *i.e.*, conformations **2–6**, which are less stable than **1** by 22.1, 60.9, 58.3, 84.5, and 121.5 kJ/mol, respectively (Table 2 and Figure 2). Figure 2 shows that there is no deviation from planarity in any conformation of purpurin.

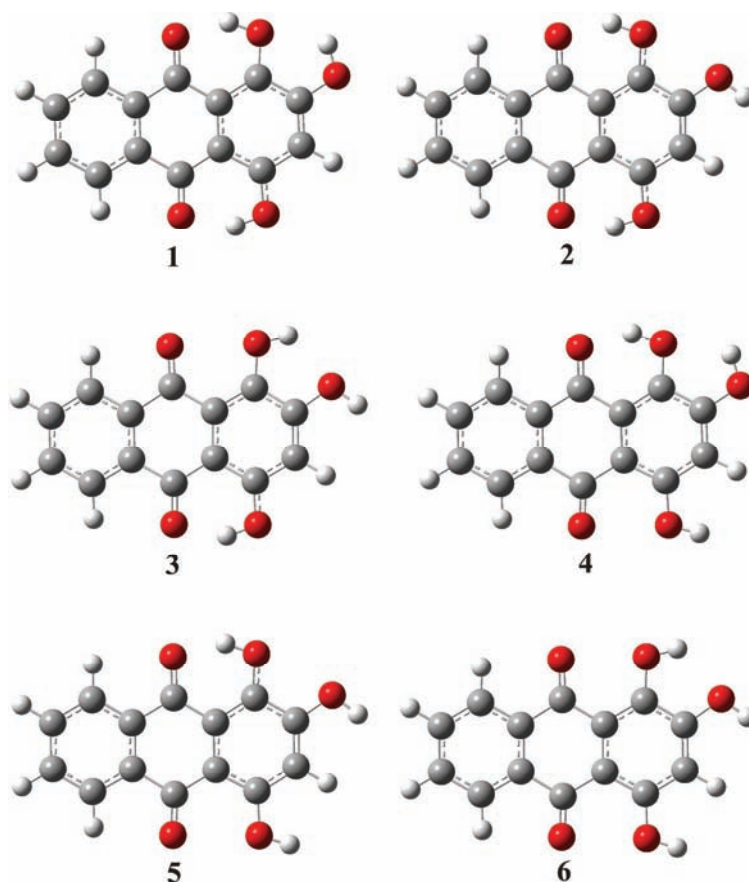


Figure 2. The optimized geometries of the six conformations for purpurin.

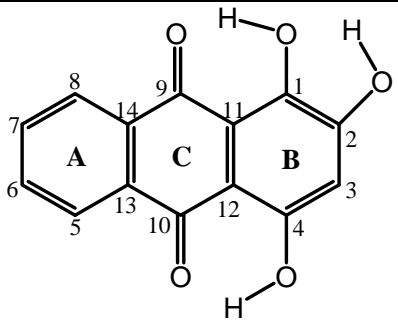
Bond lengths of the absolute minimum **1** calculated in vacuum and methanol as solvent are presented in Table 3. Table 3 shows that there are no significant differences between the geometries optimized in vacuum and methanol. In addition, it is evident that the majority of bonds in rings are longer than double bond, and shorter than single bond. The double bonds around the carbonyl groups in the ring C indicate a cross-conjugated system in which the delocalization is allowed only between A and C, or B and C, but not between A and B rings. The results of NBO analysis of **1** reveal two strong double bonds in C9-O and C10-O carbonyl groups, which form hydrogen bonds with the hydrogens of the adjacent hydroxyl groups. These hydrogen bonds have

a significant stabilizing effect, as in emodin [52] and lichexanthone [53]. Structure **6**, which lacks these hydrogen bonds, is the most unstable conformation of purpurin (Table 2).

To verify the geometry obtained by the DFT method, detailed analysis of the experimental and theoretical UV-vis and NMR spectra was performed. Both experimental and theoretical UV-vis spectra are presented in Figure 3, whereas calculated electronic transitions are given in Table 4. There is generally a very satisfactory agreement between the observed and predicted wave numbers and intensities.

The maximum for band A, whose calculated value is 467 nm, corresponds to the experimental value of 482

Table 3. Bond lengths of purpurin (**1**) and its radicals (1-OH, 2-OH and 3-OH) calculated using B3LYP/6-311+G(d,p) level of theory



Species bond	Length, nm				
	1	1 (methanol)	1-OH	2-OH	4-OH
C1–C2	0.1427	0.1424	0.1489	0.1499	0.1435
C2–C3	0.1377	0.1377	0.1366	0.1437	0.1359
C3–C4	0.1408	0.1406	0.1407	0.1376	0.1459
C4–C12	0.1411	0.1410	0.1442	0.1445	0.1478
C10–C12	0.1451	0.1450	0.1469	0.1464	0.1483
C10–C13	0.1488	0.1484	0.1473	0.1482	0.1502
C5–C13	0.1398	0.1398	0.1401	0.1399	0.1397
C5–C6	0.1390	0.1391	0.1388	0.1390	0.1390
C6–C7	0.1398	0.1397	0.1399	0.1398	0.1399
C7–C8	0.1389	0.1390	0.1390	0.1389	0.1388
C8–C14	0.1399	0.1399	0.1397	0.1399	0.1401
C13–C14	0.1408	0.1410	0.1404	0.1407	0.1405
C9–C14	0.1480	0.1478	0.1497	0.1477	0.1469
C9–C11	0.1464	0.1464	0.1488	0.1465	0.1475
C11–C12	0.1428	0.1428	0.1405	0.1422	0.1406
C1–C11	0.1392	0.1392	0.1453	0.1406	0.1415
C1–O1	0.1346	0.1344	0.1239	0.1305	0.1326
C2–O2	0.1348	0.1348	0.1323	0.1232	0.1351
C4–O3	0.1336	0.1341	0.1318	0.1338	0.1237
C9–O4	0.1243	0.1245	0.1219	0.1243	0.1245
C10–O5	0.1245	0.1249	0.1246	0.1242	0.1219
D _H (O4...H-O1)	0.1675	0.1674	–	0.1615	0.1575
D _H (O1...H-O2)	0.2116	0.2138	0.194563	–	0.2124
D _H (O5...H-O3)	0.1679	0.1662	0.157677	0.1683	–

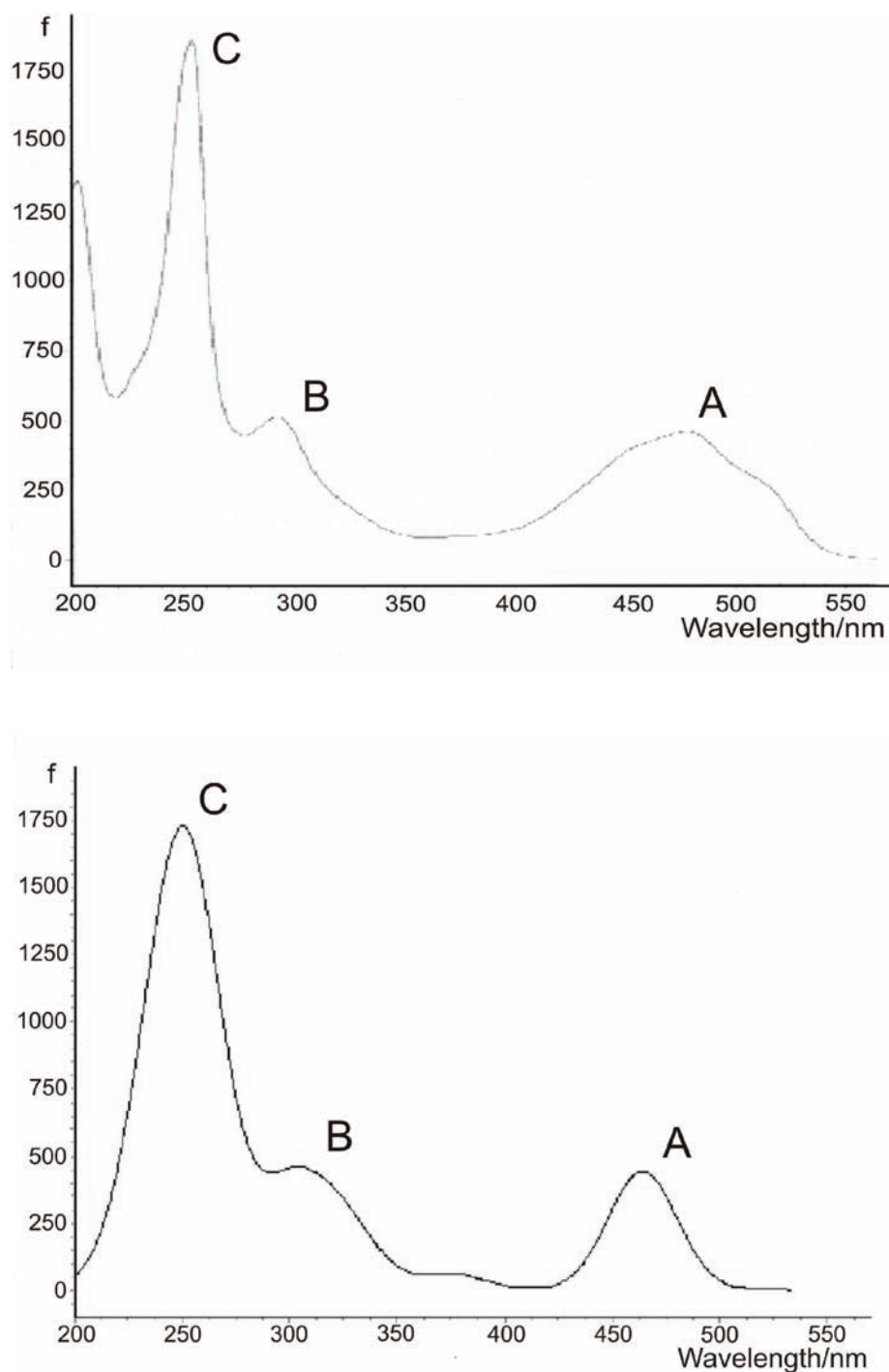


Figure 3. Experimental (top) and calculated (bottom) UV spectra for purpurin.

nm. This is essentially a HOMO–LUMO transition, involving excitation from π to π^* . The shapes of the orbitals are shown in Figure 4. They indicate that the transition is associated with significant charge-transfer from the ring B to the ring A, similar to the situation characterizing the color bands in related compounds, such as chrysazin and anthralin, and the first strong UV–vis band of the parent anthraquinone chromophore [54].

Similar charge transfer from the ring A to the ring B is observed for peak B, whose theoretical maximum is predicted at 305 nm. This band is in good agreement with the experimental polarization value of 291 nm. This transition involves excitation from HOMO-4 to LUMO. The experimental value for peak C at 252 nm is in excellent agreement with the calculated electronic transition of 254 nm. This peak mainly represents excitation from HOMO-1 to LUMO+1.

Table 4. Experimental and calculated electronic transitions for purpurin; λ – wave numbers in nm, f – oscillator strength

Case	Experimental		TD- B3LYP/6-311+G(d,p)	
	λ	λ	f	Leading configurations
A	482	466.9	0.2028	H→L(98%)
B	291	305.3	0.1675	H-4→L(81%)
C	252	254.2	0.6015	H-1→L+1(69%) H→L+2(17%)

Acker *et al.* [55] and Rice-Evans *et al.* [56], who supposed that the antioxidant properties of flavonoids could be derived just from their good delocalization possibilities. The same consideration can be applied to anthraquinones. Bearing this in mind, purpurin was screened for its antioxidant potential using the relative ability to scavenge the ABTS^{•+} radical cation generated in the aqueous phase, expressed as the Trolox equivalent antioxidant capacity (TEAC). Purpurin was found

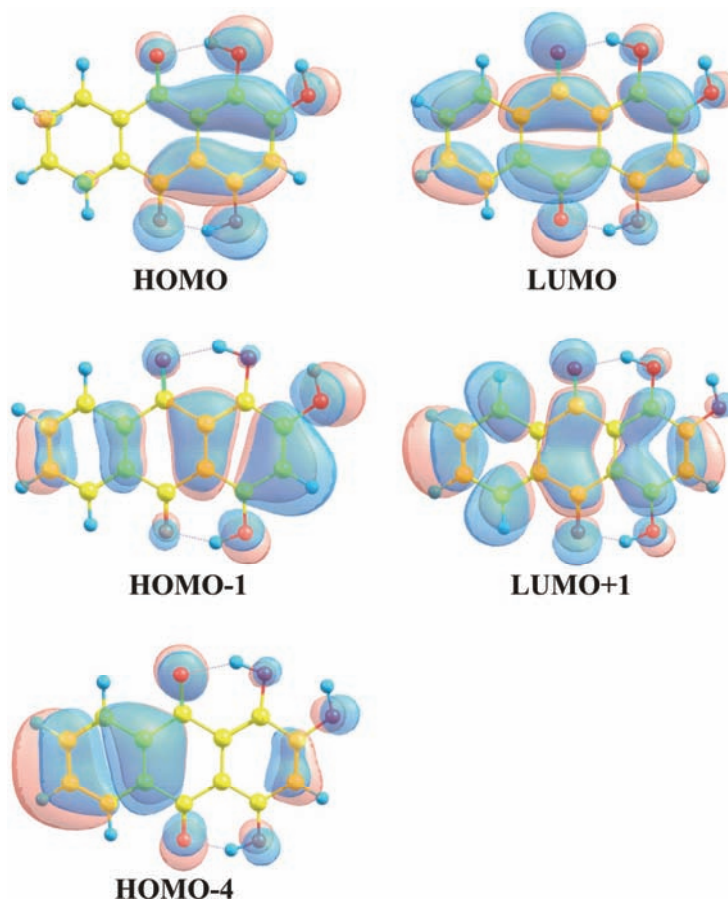


Figure 4. Selected molecular orbitals for purpurin.

The experimental and calculated ¹H- and ¹³C-NMR spectra of purpurin are presented in Table 5.

Obviously, there is a very good agreement between the experimental and theoretical values for the chemical shifts of the proton spectrum. Scaled theoretical values (scaling factor 0.953) for ¹³C chemical shifts are also in accord with the experimental data. The agreement between the experimental and theoretical results indicates that the structure of purpurin used for the UV-vis and NMR measurements corresponds to that of **1** (Figure 2).

It is well known that some anthraquinones are very good antioxidants. The structure of purpurin indicates a possibility of conjugation and antioxidant properties. This assumption is based on the suggestion of van

Table 5. Experimental and theoretical chemical shifts (in ppm) for purpurin molecule

Atom	Exp.	Calcd.	Atom	Exp.	Calcd.
C1	157.1	152.8	C12	109.7	111.3
C2	149.3	152.3	C13	133.3	141.6
C3	126.6	116.1	C14	134.5	138.9
C4	160.3	169.2	H1	13.2	13.5
C5	126.2	133.3	H2	11.6	11.3
C6	134.1	140.8	H3	6.5	6.4
C7	134.9	139.1	H4	12.9	13.4
C8	126.5	133.1	H5	8.0	8.6
C9	183.3	194.5	H6	7.8	7.5
C10	186.6	190.0	H8	7.8	7.9
C11	112.4	118.4	H8	8.1	8.7

to have the TEAC value of 1.950 ± 0.008 mM. This result is in agreement with that reported [57], and indicates that purpurin has a good antioxidant activity.

There is no detailed description of the radical cation of purpurin in literature. The radical cation formed by removing an electron from **1**, Figure 2, is planar, and hydrogen bonds are retained as in the parent molecule, contributing to further stabilization. The obtained value for the ionization potential (744.2 kJ/mol) of **1** is higher than the corresponding values for flavonoids [25], but is lower than the corresponding values for emodin and lichexanthone [52,53]. On the basis of the ionization potential value, stronger antioxidant activity of purpurin than that for emodin and lichexanthone can be expected.

It is well known that there is good correlation between antioxidant activity and *BDE* values [25,52]. For this reason, the values of *BDE* for the OH groups of purpurin were determined. The obtained results (Table 2) show that 1-OH and 2-OH groups are responsible for the antioxidant activity of purpurin. The *BDE* value for homolytic cleavage of the 1-OH bond is higher than those for dissociation of the OH groups in fisetin [58], and particularly in quercetin [25,26]. On the other hand, the obtained value is lower than the corresponding value for emodin [52].

In the text below, some properties of the radicals, formed by homolytic cleavage of the OH groups of purpurin will be discussed. Geometry optimization of the radicals was performed by starting from the optimized structure of the parent molecule **1**, and removing a hydrogen atom from the OH groups at positions 1, 2 and 4. In the further discussion, the radical formed by H-removal from the *x*-OH group of purpurin is called the *x*-OH radical ($x = 1, 2, \text{ or } 4$), for example 2-OH radical. Since the *BDE* value for 4-OH radical is significantly higher than that of 1-OH radical by almost 40 kJ/mol, only 1-OH, and 2-OH radicals will be further considered.

Inspection of the geometries of the obtained radicals shows that they retain planarity, like the parent molecule. Inspection of Table 3 allows further comment on the electronic structure of both radicals. In both radicals, complete delocalization involves only ring A, while ring B is characterized by three double bonds in 1-OH radical (C1-O, C2-C3, and C11-C12), and by two double bonds in 2-OH radical (C2-O and C3-C4). On the basis of these structural features of the radicals, it is clear that delocalization between rings C and B is restricted. A consequence of the restricted delocalization is the decreased stability of both radicals, implying that their *BDE* values are slightly higher in comparison to those obtained for the majority of the flavones [25,26,57].

To understand the relationship between the electron delocalization and the reactivity of a radical, the electron distribution in the singly occupied molecular orbital (SOMO) needs to be examined. The SOMO of the 1-OH radical (Figure 5) is mainly delocalized over carbonyl groups. As SOMO is the α -highest occupied molecular orbital, it does not describe the global electronic behavior of the radical, and its shape is not a reliable indicator for the reactivity of the purpurin radical.

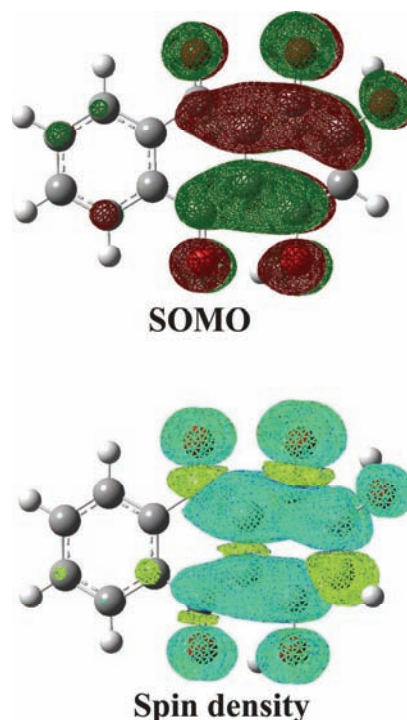
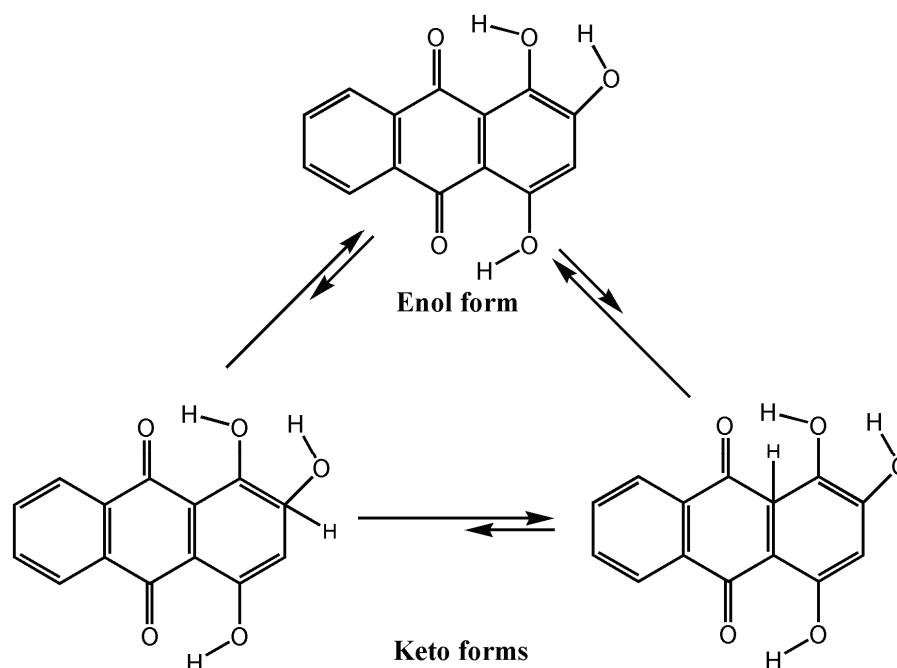


Figure 5. SOMO and spin density of the 1-OH radical.

Spin density is often considered to be a more realistic parameter, and provides a more reliable representation of the reactivity [54]. The importance of spin density for the description of flavonoids has been pointed out in the papers of Leopoldini *et al.* [25,26], and Marković *et al.* [36,52,53]. The lower the *BDE* value, the more delocalized spin density in the radical, and easier radical formation are. As this consideration can be applied to anthraquinones, the spin density in the purpurin radical was analyzed. The spin density distribution in the 1-OH radical indicates the oxygen atom bonded to C1 as the most probable radical center, followed by the adjacent carbons C2 and C11, and non-adjacent carbons C4 and C12 (Figure 5). Weak delocalization of the spin density exists over the ring C.

The OH groups of purpurin can also undergo keto-enol tautomerism. Hydrogen atom from 1-OH position can migrate to positions 2 or 11, thus yielding two tautomers (Scheme 1). The *BDE* values for the formation of the 1-OH radical by H-abstraction from the C2 and



Scheme 1. Keto-enol tautomerism in purpurin.

C11 of the keto forms of **1** were calculated (Table 2), and the values of 163.80 and 244.68 kJ/mol were obtained. These low *BDE* values indicate the relatively high capacity of H-removal from the C11, and especially from the C2 site in the keto forms. However, it should be noted that the keto forms of purpurin are less stable than the enols form, the latter being stabilized by π -conjugation in the B-ring. The differences in stability between **1**, and C2 and C11 keto forms amount to 198.35 and 117.47 kJ/mol in favor of purpurin. For instance, in the case of emodin and quercetin this difference in stability is only 61.5 and 83.8 kJ/mol [52], whereas for lichexanthone it amounts 271.9 kJ/mol [53]. These differences in stability between enol and keto forms indicate that the contribution of keto forms can be considered negligible for purpurin as a free molecule. On the other hand, it can be presumed that, in some enzymatic processes, stability difference between two forms is reduced, so that keto forms become relevant, and then H-abstraction from the C2 or C11 positions can take place easily, thereby contributing to the antioxidant properties.

CONCLUSIONS

The HPLC characterization of the extract of *Rubia tinctorum* specimens collected in central Serbia was performed. The very important anthraquinone, purpurin, was isolated and identified using HPLC, UV–vis and NMR spectral methods. The purpurin structure was determined by B3LYP/6-311+G (d,p) method. Comparison of the calculated UV–vis and ^1H - and ^{13}C -NMR spectra

with the experimental data confirmed that structure **1**, Figure 2, is likely structure of purpurin. Biological activity of anthraquinones is associated mainly with their tricyclic scaffold, but it may vary depending on the nature and/or position of substituents. On the basis of the obtained results, it is clear that purpurin, as well as its radicals, appears to be a planar tricyclic species. In spite of the planarity of the radical structure, there is no electronic delocalization between adjacent rings. It is supposed that this is one of the main reasons for higher values of *BDE* in comparison to those for flavones. In addition, the increased *BDE* values can be attributed to the cleavage of the strong hydrogen bonds, involved in the process of H-removal. Theoretical results are in accord with the experimental TEAC value. It was found that enol form is the most stable tautomer of the free molecule. Keto forms, which possess some lower *BDE* values for H-abstraction on the C2 or C11 atoms, might play a significant role in real systems, depending on the molecular environment of purpurin and on oxidative system acting on the molecule.

Acknowledgements

The authors acknowledge financial support by the Ministry of Education, Science and Technological Development of the Republic of Serbia (Grants No. 172015 and 174028).

REFERENCES

- [1] R.A. Muzychkina, Natural Anthraquinones, Biological and Physicochemical Properties, House Phasis, Moscow, 1998.

- [2] B. Li, D. M. Zhang, Y. M. Luo, X.G. Chen, Three new and antitumor anthraquinone glycosides from *Lasianthus acuminatissimus* MERR, *Chem. Pharm. Bull.* **54** (2006) 297–300.
- [3] Y. Duan, J. Yu, S. Liu, M. Ji, Synthesis of anthraquinone-ibuprofen prodrugs with hydroxyapatite affinity and anti-inflammatory activity characteristics, *Med. Chem.* **5** (2009) 577–582.
- [4] Y. Akao, Y. Nakagawa, M. Iinuma, Y. Nozawa, Anti-cancer effects of xanthenes from pericarps of mangosteen, *Int. J. Mol. Sci.* **9** (2008) 355–370.
- [5] L.G. Chen, L.L. Yang, C.C. Wang, Anti-inflammatory activity of mangostins from *Garcinia mangostana*, *Food Chem. Toxicol.* **46** (2008) 688–693.
- [6] S. Suksamrarn, O. Komutiban, P. Ratananukul, N. Chimnoi, N. Lartpornmatulee, A. Suksamrarn, Cytotoxic prenylated xanthenes from the young fruit of *Garcinia mangostana*, *Chem. Pharm. Bull.* **54** (2006) 301–305.
- [7] J. Pedraza-Chaverri, N. Cárdenas-Rodríguez, M. Orozco-Ibarra, J.M. Pérez-Rojas, Medicinal properties of mangosteen (*Garcinia mangostana*), *Food Chem. Toxicol.* **46** (2008) 3227–3239.
- [8] G. Gopalakrishnan, B. Banumathi, G.J. Suresh, evaluation of the antifungal activity of natural xanthenes from *Garcinia mangostana* and their synthetic derivatives, *Nat. Prod.* **60** (1997) 519–524.
- [9] T.N. Manojlović, S. Solujić, S. Sukdolak, Antimicrobial activity of an extract and anthraquinones from *Caloplaca schaeferi*, *Lichenologist* **34** (2002) 83–85.
- [10] J.C. Cyoug, T. Matsumoto, K. Arakawa, H. Kiyohara, H. Yamoda, Y. Otsuka, Anti-*Bacteroides fragilis* substance from Rhubarb, *J. Ethnopharmacol.* **19** (1987) 279–283.
- [11] G.C. Yen, P.D. Duh, D.Y. Chuang, Antioxidant activity of anthraquinones and anthrone, *Food Chem.* **70** (2000) 437–441.
- [12] M.M.M. Pinto, M.E. Souza, M.S.J. Nascimento, Xanthone derivatives: New insights in biological activities, *Curr. Medic. Chem.* **12** (2005) 2517–2538.
- [13] G.C.H. Derksen, H.A.G. Niederländer, T.A. van Beek, Analysis of anthraquinones in *Rubia tinctorum* L. by liquid chromatography coupled with diode-array UV and mass spectrometric detection, *J. Chromatogr., A* **978** (2002) 119–127.
- [14] J.N. Hao, M.P. Huang, H. Lee, Structure-activity relationships of anthraquinones as inhibitors of 7-ethoxycoumarin *O*-deethylase and mutagenicity of 2-amino-3-methylimidazo [4,5-f] quinoline, *Mutat. Res.* **328** (1995) 183–191.
- [15] T.H. Marczylo, T. Hayatsu, S. Arimoto-Kobayashi, M. Tada, K. Fujita, T. Kamataki, K. Nakayama, H. Hayatsu, Protection against the bacterial mutagenicity of heterocyclic amines by purpurin, a natural anthraquinone pigment, *Mutat. Res.* **444** (1999) 451–461.
- [16] T.H. Marczylo, S. Arimoto-Kobayashi, H. Hayatsu, Protection against Trp-P-2 mutagenicity by purpurin: mechanism of *in vitro* antimutagenesis, *Mutagenesis* **15** (2000) 223–228.
- [17] N.T. Manojlović, S. Solujić, S. Sukdolak, M. Milošev, Antifungal activity of *Rubia tinctorum*, *Rhamnus frangula* and *Caloplaca cerina*, *Fitoterapia* **76** (2005) 244–246.
- [18] J. Westendorf, W. Pfau, A. Schulte, Carcinogenicity and DNA adduct formation observed in ACI rats after long-term treatment with madder root, *Rubia tinctorum* L., *Carcinogenesis* **19** (1998) 2163–2168.
- [19] B. Blömeke, B. Poginsky, C. Schmutte, H. Marquardt, J. Westendorf, Formation of genotoxic metabolites from anthraquinone glycosides, present in *Rubia tinctorum* L., *Mutat. Res.* **265** (1992) 263–272.
- [20] P. Bányai, I.N. Kuzovkina, L. Kursinszki, É. Szőke, HPLC Analysis of Alizarin and Purpurin Produced by *Rubia tinctorum* L., *Hairy Root Cultures* **63** (2006) 111–114.
- [21] M.J. Mayer, Proton-coupled electron transfer: A Reaction Chemist's View, *Annu. Rev. Phys. Chem.* **55** (2004) 363–390.
- [22] G.A. DiLabio, R.E. Johnson, Lone pair- π and π - π interactions play an important role in proton-coupled electron transfer reactions, *J. Am. Chem. Soc.* **129** (2007) 6199–6203.
- [23] G.A. DiLabio, K.U. Ingold, A theoretical study of the iminoxyl/oxime self-exchange reaction. A five-center, cyclic proton-coupled electron transfer, *J. Am. Chem. Soc.* **127** (2005) 6693–6699.
- [24] M. Sjödin, S. Styring, B. Åkermark, L. Sun, L. Hammarström, Proton-coupled electron transfer from tyrosine in a tyrosine-ruthenium-tris-bipyridine complex: Comparison with tyrosine oxidation in photosystem II, *J. Am. Chem. Soc.* **122** (2000) 3932–3936.
- [25] M. Leopoldini, I.P. Pitarch, N. Russo, M. Toscano, Structure, conformation, and electronic properties of apigenin, luteolin, and taxifolin antioxidants. A First principle theoretical study, *J. Phys. Chem., A* **108** (2004) 92–96.
- [26] M. Leopoldini, T. Marino, N. Russo, M. Toscano, Density functional computations of the energetic and spectroscopic parameters of quercetin and its radicals in the gas phase and in solvent, *Theor. Chem. Acc.* **111** (2004) 210–216.
- [27] M. Lucarini, F. G. Pedulli, M. Guerra, A critical evaluation of the factors determining the effect of intramolecular hydrogen bonding on the O-H bond dissociation enthalpy of catechol and of flavonoid antioxidants, *Chem-Eur. J.* **10** (2004) 933–939.
- [28] K. Lemaska, H. Szymusiak, B. Tyrakowska, R. Zieliski, A.E.M.F. Soffers, I.M.C.M. Rietjens, The influence of pH on antioxidant properties and the mechanism of antioxidant action of hydroxyflavones, *Free Radical Bio. Med.* **31** (2001) 869–881.
- [29] P. Trouillas, C. Fagnère, R. Lazzaroni, A.C. Calliste, A. Marfak, L.J. Duroux, A theoretical study of the conformational behavior and electronic structure of taxifolin correlated with the free radical-scavenging activity, *Food Chem.* **88** (2004) 571–582.
- [30] H.Y. Zhang, On the effectiveness of the EPR radical equilibration technique in estimating O–H bond dissociation enthalpies of catechols and other complex polyphenols, *New J. Chem.* **28** (2004) 1284–1285.

- [31] H.Y. Zhang, Y.M. Sun, X.L. Wang, Substituent effects on O–H bond dissociation enthalpies and ionization potentials of catechols: A DFT study and its implications in the rational design of phenolic antioxidants and elucidation of structure–activity relationships for flavonoid antioxidants, *Chem-Eur. J.* **9** (2003) 502–508.
- [32] K.I. Priyadarsini, D.K. Maity, G.H. Naik, M.S. Kumar, M.K. Unnikrishnan, J.G. Satav, Role of phenolic O–H and methylene hydrogen on the free radical reactions and antioxidant activity of curcumin, *Free Radical Bio. Med.* **35** (2003) 475–484.
- [33] N. Russo, M. Toscano, N. Uccella, Semiempirical molecular modeling into quercetin reactive site: Structural, conformational, and electronic features, *J. Agric. Food Chem.* **48** (2000) 3232–3237.
- [34] S.J. Wright, R.E. Jonhson, A.G. DiLabio, Predicting the activity of phenolic antioxidants: Theoretical method, analysis of substituent effects, and application to major families of antioxidants, *J. Am. Chem. Soc.* **123** (2001) 1173–1183.
- [35] Y.H. Zhang, M.Y. Sun, Z.D. Chen, O–H bond dissociation energies of phenolic compounds are determined by field/inductive effect or resonance effect? A DFT study and its implication, *QSAR* **20** (2001) 148–152.
- [36] Z.S. Marković, J.M.D. Marković, Č. Doličanin, A PM6 study on the reactivity of OH groups in fisetin: Structural and electronic features of fisetin radicals, *J. Ser. Soc. Comp. Mech.* **3** (2009) 43–55.
- [37] P. Mulder, G.H. Korth, U.K. Ingold, Why quantum-thermochemical calculations must be used with caution to indicate a promising lead antioxidant, *Helv. Chim. Acta* **88** (2005) 370–374.
- [38] R.H. Thomson, *Natural Occurring Quinones*, Academic Press, London, New York, 1971.
- [39] Gaussian 09, Revision A.1-SMP, Gaussian Inc., 2009, Wallingford, CT.
- [40] A. D. Becke, Density-functional thermochemistry. 2. The effect of the Perdew-Wang generalized-gradient correlation correction, *J. Chem. Phys.* **97** (1992) 9173–9177.
- [41] A.D. Becke, Density-functional thermochemistry. 3. The role of exact exchange, *J. Chem. Phys.* **98** (1993) 5648–5652.
- [42] C. Lee, W. Yang, R.G. Parr, Development of the Colle-Salvetti correlation-energy formula into a functional of the electron density, *Phys. Rev., B* **37** (1988) 785–789.
- [43] S. Miertuš, S. Scrocco, J. Tomasi, Electrostatic interaction of a solute with a continuum. A direct utilization of AB initio molecular potentials for the prevision of solvent effects, *Chem. Phys.* **55** (1981) 117–129.
- [44] J. Tomasi, B. Mennucci, R. Cammi, Quantum mechanical continuum solvation models, *Chem. Rev.* **105** (2005) 2999–3094.
- [45] N.M. O'boyle, A.L. Tenderholt, K.M. Langner, cclib: A library for package-independent computational chemistry algorithms, *J. Comp. Chem.* **29** (2008) 839–845.
- [46] G.A. Zhurko, D. A. Zhurko, Chemcraft 1.6, Chemcraft graphical program for working with quantum chemistry results, 2009. Available from: <http://www.chemcraft-prog.com> (accessed on Feb, 2013).
- [47] R. Ditchfield, Self-consistent perturbation theory of diamagnetism, *Mol. Phys.* **27** (1974) 789–807.
- [48] K. Wolinski, J. Hilton, F.P. Pulay, Efficient implementation of the gauge-independent atomic orbital method for NMR chemical shift calculations, *J. Am. Chem. Soc.* **112** (1990) 8251–8260.
- [49] J.P. Merrick, D. L. Moran, L. Radom, An evaluation of harmonic vibrational frequency scale factors, *J. Phys. Chem.* **111** (2007) 11683–11700.
- [50] J.P. Foster, F. Weinhold, Natural hybrid orbitals, *J. Am. Chem. Soc.* **102** (1980) 7211–7218.
- [51] C.H.G. Derksena, A.G.H. Niederlanderb, A.T. van Beek, Analysis of anthraquinones in *Rubia tinctorum* L. by liquid chromatography coupled with diode-array UV and mass spectrometric detection, *J. Chromatog., A* **978** (2002) 119–127.
- [52] S.Z. Marković, T.N. Manojlović, DFT study on the reactivity of OH groups in emodin: structural and electronic features of emodin radicals, *Monatsh. Chem.* **140** (2009) 1311–1318.
- [53] S.Z. Marković, T.N. Manojlović, Analytical characterization of lichexanthone in lichen: HPLC, UV spectroscopic, and DFT analysis of lichexanthone extracted from *Laurera benguelensis* (Mull. Arg.) Zahlbr, *Monatsh. Chem.* **141** (2010) 945–952.
- [54] S. Møller, K.B. Andersen, J. Spanget-Larsen, J. Waluk, Excited-state intramolecular proton transfer in anthraxlin: Quantum chemical calculations and fluorescence spectra, *Chem. Phys. Lett.* **291** (1998) 51–56.
- [55] S.A.B.E. van Acker, M.J. Groot, W.J.F. van der Vijgh, M.N.J.L. Tromp, G.F. den Kelder, E.J.F. van der Vijgh, A. Bast, A Quantum chemical explanation of the antioxidant activity of flavonoids, *Chem. Res. Toxicol.* **9** (1996) 1305–1312.
- [56] C.A. Rice-Evans, N.J. Miller, G. Paganga, Structure-antioxidant activity relationships of flavonoids and phenolic acids, *Free Radic. Biol. Med.* **20** (1996) 933–956.
- [57] Y.Z. Cai, M. Sun, J. Xing, Q. Luo, H. Corke, Structure–radical scavenging activity relationships of phenolic compounds from traditional Chinese medicinal plants, *Life Sciences* **78** (2006) 2872–2888.
- [58] S.Z. Marković, J.M. Dimitrić-Marković, Č.B. Doličanin, Mechanistic pathways for the reaction of quercetin with hydroperoxy radical, *Theor. Chem. Acc.* **127** (2010) 69–80.

IZVOD

HPLC, UV–vis, NMR spektroskopska i DFT karakterizacija purpurina izolovanog iz *Rubia tinctorum* L.Zoran S. Marković¹, Nedeljko T. Manojlović², Svetlana R. Jeremić², Miroslav Živić³¹*Državni univerzitet u Novom Pazaru, Departman za hemijsko-tehnološke nauke, Novi Pazar, Srbija*²*Univerzitet u Kragujevac, Fakultet medicinskih nauka, Departman za farmaciju, Kragujevac, Srbija*³*Univerzitet u Beogradu, Biološki fakultet, Beograd, Srbija*

(Naučni rad)

Purpurin (1,2,4-trihidroksiantrahinon), prirodni pigment antrahinonske strukture koji se nalazi u korenu biljke *Rubia tinctorum*, izolovan je iz ove biljke, prečišćen i okarakterisan primenom HPLC hromatografije, UV–vis i NMR spektroskopije. Geometrije konformera purpurina optimizovane su korišćenjem B3LYP/6-311+G(d,p) nivoa teorije. Nađeno je da svi konformeri purpurina imaju slične energije, kao i da odgovarajući radikal purpurina ima planarnu strukturu. U svetlu ove planarnosti, zaključeno je da ne postoji značajna delokalizacija elektrona iznad prstenova A i C. Antioksidativne osobine purpurina određene su kolorimetrijski, primenom Troloksa, čiji je oksidativni kapacitet uzet za ekvivalent i teorijski, primenom *BDE* (eng. Bond Dissociation Enthalpy) metode. Obe ove metode su potvrdile odličan antioksidativni kapacitet purpurina.

Ključne reči: *Rubia tinctorum* • HPLC-UV
• Antioksidativna aktivnost • DFT studija